Electrical Power and Energy Systems 87 (2017) 27–42

Contents lists available at ScienceDirect

Electrical Power and Energy Systems

journal homepage: www.elsevier.com/locate/ijepes

Decentralized reactive power control of distributed PV and wind power generation units using an optimized fuzzy-based method

F. Rezaei [1], S. Esmaeili *,[2]

Shahid Bahonar University of Kerman, Kerman, Iran

ARTICLE INFO

Article history:
Received 25 October 2015
Received in revised form 7 September 2016
Accepted 28 October 2016

Keywords:
Distributed generation
Distribution system
Fuzzy logic
Mathematical optimization
Reactive power control and coordination

ABSTRACT

The presence of power electronic-based wind turbines and photovoltaic systems in distribution networks has provided distribution companies an opportunity to implement voltage control through using the reactive power of these systems. In this paper, a decentralized method based on fuzzy logic is proposed to control the reactive power of distributed generations (DGs) regarding the technical constraints. The fuzzy system is optimized by gradient descent algorithm (GDA) and then implemented on various DG technologies including a photovoltaic (PV) system, permanent magnet synchronous generator (PMSG) wind turbine and also a doubly fed induction generator (DFIG) wind turbine. The system under study is tied to a real distribution network. Having simulated the system, the paper shows that the fuzzy system can appropriately determine the desired reactive power that should be produced by each DG based on the voltage variation of the bus at which the DG is connected. Furthermore, a centralized voltage control is also applied to the same network to verify the performance of the method proposed. The verification indicates that the method is capable of finding the near-optimal solution. A scenario in which an unwanted conflict appears in the DGs' function is defined in detail and then a strategy is presented to resolve the situation. In addition to this, the coordination between the stator of the wind turbines and grid side converter (GSC) is examined. To investigate the robustness of the proposed method in different distribution networks, simulation results are also presented for IEEE 33-bus distribution test system. The numerical results show that the fuzzy system can effectively control the voltage of the DG connection bus.

1. Introduction

Most of the distributed generations (DGs) use inverters to connect to the power grid such as photovoltaic (PV) systems, wind turbines with full-power converters and wind turbines made up with doubly fed induction generators (DFIG). These DG technologies have become very popular for their benefits and now they are a part of the distribution systems [1]. DGs can supply the load active and reactive power locally, which results in a reduction in line losses [2]. Also, voltage and stability of the power system can be improved by integrating DG into the power grid [3]. An interesting feature of inverter-based DGs is their capability of reactive power control and some grid codes now require that PV systems and wind turbines participate in reactive power control of the power system [4]. To comply with new grid codes, solar inverter manufacturers are presenting their photovoltaic inverters with reactive power control capability. These inverters have different control modes and can even produce reactive power at night [5]. Application of PV systems for voltage regulation at night is proposed in the literature. PV systems can be used to regulate the voltage of the connection bus such as a static synchronous compensator (STATCOM) [6]. Similarly, wind turbines are capable of supporting reactive power to the grid when the wind turbines are generating active power or even when the wind speed drops below the cut-in threshold and they are not generating active power [7,8]. Wind turbines can provide the optimum reactive power by means of their converters. The reactive power capability of DGs is limited by several factors which are discussed in the papers [4,9,10]. Reactive power capability of DG increases with the decrease in its active power. Larger reactive power capability means larger inverters, and certainly a larger investment.

Reactive power control of the renewable energy-based DGs not only helps the power grid, it can also mitigate the voltage rise and voltage fluctuations due to the high penetration of DGs. In the high R/X distribution system, active power curtailment is suggested to avoid voltage rise of DGs [11]. However, active power curtailment

* Corresponding author.
E-mail addresses: f.rezaei@eng.uk.ac.ir (F. Rezaei), s_esmaeili@uk.ac.ir (S. Esmaeili).
[1] Msc student, Department of Electrical Engineering.
[2] Associate Professor, Department of Electrical Engineering.

http://dx.doi.org/10.1016/j.ijepes.2016.10.015
0142-0615/

Nomenclature

b_{ij}, c_{ij}	points of the membership functions
c_1, c_2	learning coefficients
$\cos(\varphi)$	DG power factor
E_{loss}	active energy consumed by the lines
f	grid frequency
F	objective function
G_{best}	global best position
I_{INV}	inverter current
I_R	rotor current
I_S	stator current
P_{best}	personal best position
P_{DG}	active power of DG
P_{GSC}	active power of the grid side converter
P_L	active load demand at the connection bus
P_R	active power of the rotor
P_S	active power of the stator
$Q_{I,max}$	reactive power limit related to inverter current
$Q_{DG,max}$	reactive power capability of DG
$Q_{GSC,max}$	reactive power capability of grid side converter
Q_L	reactive load at connection bus
Q_{loss}	reactive energy consumed by the lines
$Q_{RC,max}$	reactive power limit related to rotor current
$Q_{S,max}$	reactive power capability of stator
$Q_{SC,max}$	reactive power limit related to stator current
$Q_{V,max}$	reactive power limit related to inverter voltage
r_1, r_2	random numbers between 0 and 1
S	slip of the doubly fed induction generator
S_{GSC}	apparent power of grid side converter
Vel_i	velocity of particle i
V_{CB}	voltage at connection bus
V_{INV}	inverter voltage
VR	voltage profile regulation
X_{EQV}	total equivalent reactance
X_i	position of particle i
X_M	mutual reactance
X_S	stator leakage reactance
ω	inertia weight
η	step size in gradient descent algorithm

is not appealing to owners of renewable energy power plants as the loss of unproduced power is not economical for them [12]. Another solution is reactive power control of PV systems and wind turbines by means of their inverters. These solutions are either centralized or decentralized. Centralized methods require extensive data from the distribution system usually to determine an optimum response. A centralized control method is proposed in [10] to improve the voltage profile and to decrease system losses. A particle swarm optimization (PSO) algorithm is used to determine the optimal reactive power output of wind turbines and power grid reconfiguration, simultaneously. In [13], optimal coordination of PV systems and transformer tap changers are considered based on centralized information of the distribution system. Another centralized method is presented in [14] to coordinate the reactive power of PV systems with capacitor banks and tap changers with the aim to improve voltage profile and reduce power losses.

The centralized control methods need high investment in reliable communication channels and sensors, also communication malfunction or slow response of centralized methods could be a problem, whereas decentralized methods do not require extensive communications infrastructure. However, decentralized methods are unable to reach the global optimum since they are implemented on the base of local data. A decentralized voltage control method based on sensitivity analysis is proposed in [15,16]. In this method, the optimal reactive power of DG is obtained by using the sensitivity of voltage at a specific bus to the active and reactive power of DGs. In [17], DG's reactive power output is considered by using a fuzzy logic-based voltage control method. The fuzzy control system provides a gentle response with a lower reactive power consumption than the sensitivity-based method. The design of fuzzy control system is not dependent on the knowledge of distribution system parameters and it can be easily implemented without investment in communication infrastructure.

To increase the reactive power capability of DFIG wind turbine, several researchers have considered the reactive power support of the grid side converter (GSC) [18,19]. They have proposed a strategy to coordinate stator and GSC in reactive power control. One strategy defines DFIG stator as the main supply of reactive power and the GSC of DFIG wind turbine as the second voltage controller. When the optimum reactive power exceeds the stator's reactive power limits, GSC provides the excess reactive power required to regulate the bus voltage.

Simultaneous responses of DGs and voltage regulating devices for regulating voltage profile might result in operational conflicts [20]. Also, "hunting behavior" between DGs with mutual interactions are possible [21]. Therefore, coordination of DGs and voltage regulating devices might be required in distribution systems. Ref. [20] proposes to consider time delays for DGs and voltage regulating devices such as OLTC and SVRs to avoid simultaneous operations.

In this paper, reactive power limiting factors of PV systems, the PMSG wind turbines and also DFIG wind turbines are discussed and their reactive power capability is determined. Furthermore, Reactive power capability of the GSC is introduced and coordinated reactive power control of GSC and DFIG stator is investigated. A decentralized voltage control method based on fuzzy logic is presented and the gradient descent algorithm (GDA) is proposed to optimize the fuzzy system. The proposed method is implemented on DGs to determine the desired reactive power that should be produced by each DG by considering DG's reactive power capability. A centralized voltage control method based on the PSO is also applied to the distribution network to verify the performance of the proposed decentralized method. Finally, the simulation results and discussions are presented.

2. Reactive power capability of DGs and power flow modeling

PV systems and wind turbines have limited capabilities to supply or absorb reactive power. In the following, reactive power limiting factors of these technologies are presented.

2.1. Reactive power limiting factors of DGs with full-power converters

Fig. 1 shows a schematic of DG with full-power converters. The generator in Fig. 1 refers to either permanent magnet synchronous generator (PMSG) of the wind turbine or PV arrays in this paper. PMSG wind turbine and PV system have the same reactive power limiting factors. All of produced active and reactive power is transferred to the grid through the inverter. Maximum inverter current ($I_{INV,max}$) and maximum inverter voltage ($V_{INV,max}$) impose reactive power constraints of $Q_{I,max}$ and $Q_{V,max}$ respectively as follows [4,9]:

$$Q_{I,max} = \sqrt{(V_{CB} I_{INV,max})^2 - P_{DG}^2} \quad (1)$$

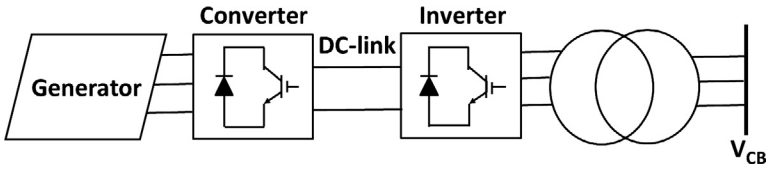

Fig. 1. DG with full-scale power converters.

$$Q_{V,max} = \sqrt{\left(\frac{V_{CB}V_{INV,max}}{X_{EQV}}\right)^2 - P_{DG}^2} - \frac{V_{CB}^2}{X_{EQV}} \quad (2)$$

where V_{CB} is voltage at the DG connection bus, P_{DG} is DG active power and X_{EQV} is the total equivalent reactance including step up transformer and the grid filters reactance.

Therefore, the reactive power capability of DG ($Q_{DG,max}$) is minimum of $Q_{I,max}$ and $Q_{V,max}$:

$$Q_{DG,max} = min\{Q_{I,max}, Q_{V,max}\} \quad (3)$$

Larger $I_{INV,max}$ and $V_{INV,max}$ result in larger reactive power capability but also increase in the price of the inverter. Inverter current (I_{INV}) is related to P_{DG} and reactive power (Q_{DG}) as follows:

$$I_{INV} = \frac{\sqrt{P_{DG}^2 + Q_{DG}^2}}{V_{CB}} \quad (4)$$

$I_{INV,max}$ is obtained when P_{INV} and Q_{INV} are at the rated value and V_{CB} is minimum:

$$I_{INV,max} = \frac{\sqrt{(P_{DG,rated})^2 + (Q_{DG,rated})^2}}{V_{CB,min}} \quad (5)$$

Considering that:

$$Q_{DG,rated} = P_{DG,rated} \times \tan(\varphi_{DG,rated}) \quad (6)$$

and:

$$S_{DG,base} = P_{DG,rated} \quad (7)$$

where $\cos(\varphi_{DG,rated})$ is rated power factor (pf) and $S_{DG,base}$ is base megavolt ampere of DG. According to Eqs. (5)–(7) the p.u value of $I_{INV,max}$ is calculated as:

$$I_{INV,max} = \frac{\sqrt{1 + \tan^2(\varphi_{DG,rated})}}{V_{CB,min}} \quad (8)$$

According to [9], V_{INV} is given by:

$$V_{INV} = \frac{X_{EQV}}{V_{CB}}\sqrt{P_{DG}^2 + \left(P_{DG} \times \tan\varphi_{DG,rated} + \frac{V_{CB}^2}{X_{EQV}}\right)^2} \quad (9)$$

V_{INV} is maximum when P_{DG}, V_{CB} and grid frequency are maximum. Therefore $V_{INV,max}$ in p.u is:

$$V_{INV,max} = \frac{f_{max} \times X_{EQV}}{V_{CB,max}}\sqrt{1 + \left(\tan\varphi_{DG,rated} + \frac{V_{CB,max}^2}{f_{max} \times X_{EQV}}\right)^2} \quad (10)$$

Inverter maximum current and voltage are related to rated power factor of DG by Eqs. (8) and (10).

2.2. Reactive power limiting factors of wind turbines with doubly fed induction generator

A wind turbine made up with DFIG is shown in Fig. 2. The rotor of DFIG is connected to the grid via two converters and the stator of DFIG is coupled directly to the grid. Both rotor and stator deliver power to the grid and the total active power of DG is:

$$P_{DG} = P_S + P_R \quad (11)$$

Table 1
DGs parameters.

Parameter	Value
PV system	
P_{rated}	976 kW
$I_{INV,max}$	1.17 p.u
$V_{INV,max}$	1.17 p.u
X_{EQV}	0.3 p.u
PMSG wind turbine	
P_{rated}	200 kW
$I_{INV,max}$	1.17 p.u
$V_{INV,max}$	1.17 p.u
X_{EQV}	0.3 p.u
V_I	3.5 m/s
V_R	12 m/s
DFIG wind turbine	
P_{rated}	1500 kW
$I_{S,max}$	1 p.u
X_S	0.167 p.u
X_M	5.419 p.u
S	−0.167 to 0.2
S_{GSC}	375 kVA
V_I	3.5 m/s
V_R	12 m/s

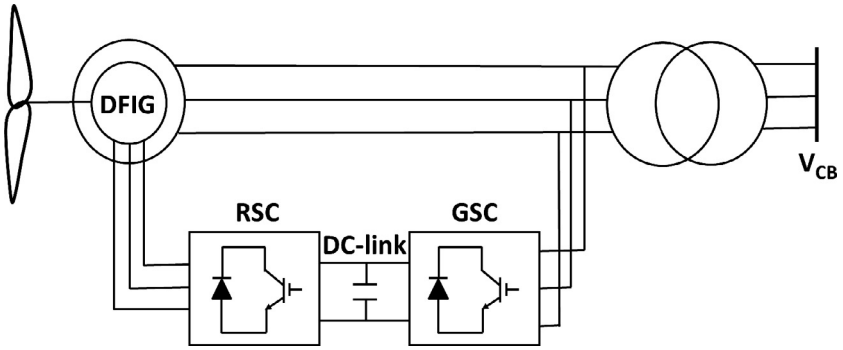

Fig. 2. Wind turbine made up with DFIG.

where P_S and P_R are the stator and rotor active powers respectively. Maximum allowed stator current ($I_{S,max}$) and maximum allowed rotor current ($I_{R,max}$) impose reactive power constraints of $Q_{SC,max}$ and $Q_{RC,max}$ respectively [10]:

$$\left(\frac{P_{DG}}{1-S}\right)^2 + Q_{SC,max}^2 = (V_{CB}I_{S,max})^2 \tag{12}$$

$$\left(\frac{P_{DG}}{1-S}\right)^2 + \left(Q_{RC,max} + \frac{V_{CB}^2}{X_S+X_M}\right)^2 = \left(\frac{X_M}{X_S+X_M}V_{CB}I_{R,max}\right)^2 \tag{13}$$

where X_S is stator leakage reactance, X_M is mutual reactance, and S is the slip. The stability limit of the DFIG wind turbine is also taking account in reactive power limits, which means that the DFIG wind turbine becomes unstable if it absorbs reactive power more than $\frac{V_{CB}^2}{X_S+X_M}$. Therefore the reactive power capability ($Q_{S,max}$) is the minimum of $Q_{SC,max}$, $Q_{RC,max}$, and the stability limit $\left(\frac{V_{CB}^2}{X_S+X_M}\right)$ [10]:

$$Q_{S,max} = min\left\{Q_{SC,max}, Q_{RC,max}, \frac{V_{CB}^2}{X_S+X_M}\right\} \tag{14}$$

To increase the reactive power support from DFIG wind turbine, reactive power capability of GSC ($Q_{GSC,max}$) is also considered. So $Q_{DG,max}$ in every moment (t) is:

$$Q_{DG,max}(t) = Q_{S,max}(t) + Q_{GSC,max}(t) \tag{15}$$

$Q_{GSC,max}$ is related to rated apparent power of the GSC ($S_{GSC,rated}$) and active power of GSC (P_{GSC}) [22]:

$$Q_{GSC,max} = \sqrt{(S_{GSC,max})^2 - P_{GSC}^2} \tag{16}$$

where P_{GSC} is:

$$P_{GSC} = P_{DG} \times \left(\frac{S}{S-1}\right) \tag{17}$$

2.3. Design values and reactive power capability curves

DGs performance parameters are given in Table 1. It is assumed that f_{max} = 1.01 p.u, $V_{CB,min}$ = 0.9 p.u, $V_{CB,max}$ = 1.05 p.u [9]. PV system and PMSG wind turbine are designed to be able to work at 0.95 power factor and DFIG wind turbine at unity power factor. Therefore, $I_{INV,max}$ and $V_{INV,max}$ are calculated using Eqs. (8), (10) and the reactive power capabilities of DGs are obtained. Fig. 3 shows the reactive power characteristic of PV system, the PMSG wind turbine, and stator and the GSC of DFIG wind turbine at V_{CB} = 1 p.u. It can be observed from Fig. 3 that reactive power capability of DG increases as DG active power decreases. Therefore, at low wind speeds/low solar radiation, wind turbines/PV systems have their largest reactive power capability.

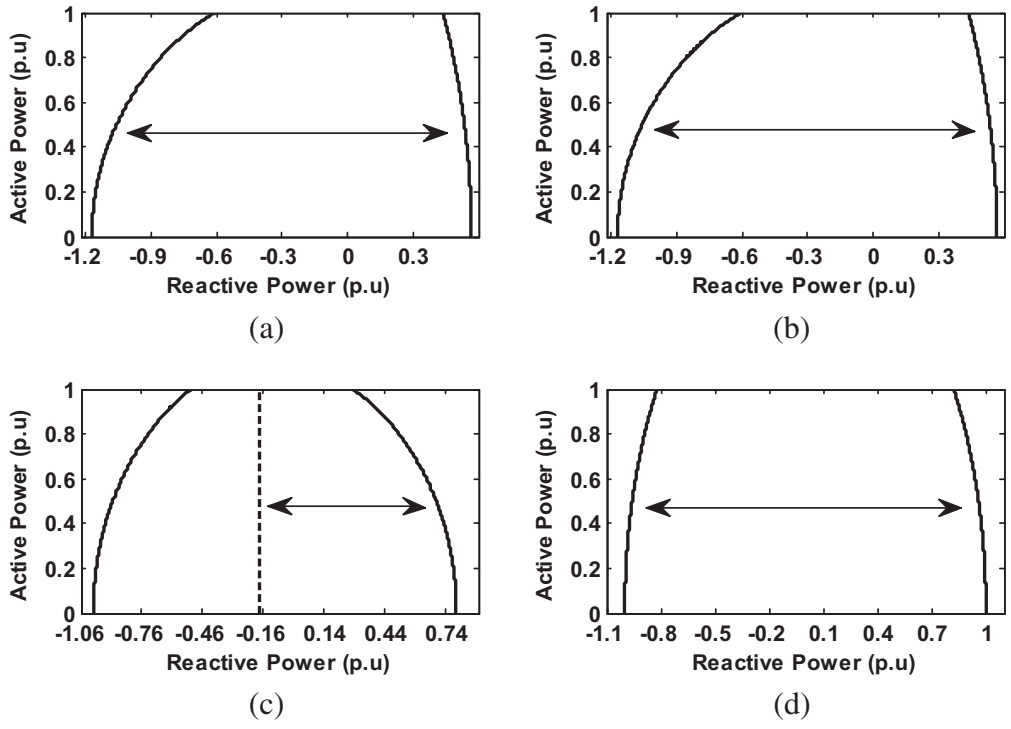

Fig. 3. DG capability curves: (a) PV system, (b) PMSG wind turbine, (c) DFIG wind turbine, and (d) GSC.

Table 2
Fuzzy rules.

Voltage variation	Voltage				
	Very high	High	Optimum	Low	Very low
Negative	High absorp.	Absorp.	Gen.	Gen.	High gen.
Zero	High absorp.	Absorp.	Zero	Gen.	High gen.
Positive	High absorp.	Absorp.	Absorp.	Gen.	High gen.

2.4. Power flow modeling of DGs

DGs can be modeled as PQ or PV buses in power flow studies. Since DGs are small-capacity units, their voltage regulation capability is limited compared with conventional power plants. If DG is modeled as PV bus, it may reach its reactive power limits and the PV bus turns into a PQ bus. In [23,24] DGs are considered as negative loads in an optimal allocation problem. In this model, DG is a constant active and reactive power generating source. In the current paper, DGs are considered as negative PQ load and at each time step P_{DG} is updated and Q_{DG} is determined by the proposed fuzzy reactive power control method. Therefore, active and reactive load at the connection bus (P_L and Q_L) are modified as given in Eqs. (18) and (19).

$$P_L(t) = P_L(t) - P_{DG}(t) \tag{18}$$

$$Q_L(t) = Q_L(t) - Q_{DG}(t) \tag{19}$$

3. Reactive power control

A decentralized method based on Mamdani fuzzy inference system is used in this paper to determine the optimum reactive power output of DG units. The PSO is also used to verify the performance of the proposed fuzzy-based method.

3.1. Fuzzy control system

The fuzzy system receives voltage and voltage variation at DG connection bus and calculates the reactive power output of DG by using the fuzzy rules that are defined in Table 2. Fuzzy rules are set to regulate the connection bus voltage at 1 p.u. As shown in Fig. 4, two inputs and one output are defined for the fuzzy system with the triangular- shaped membership functions. Membership functions of input 1 and input 2 are the same for all DGs but since DGs have different reactive power capabilities, the fuzzy

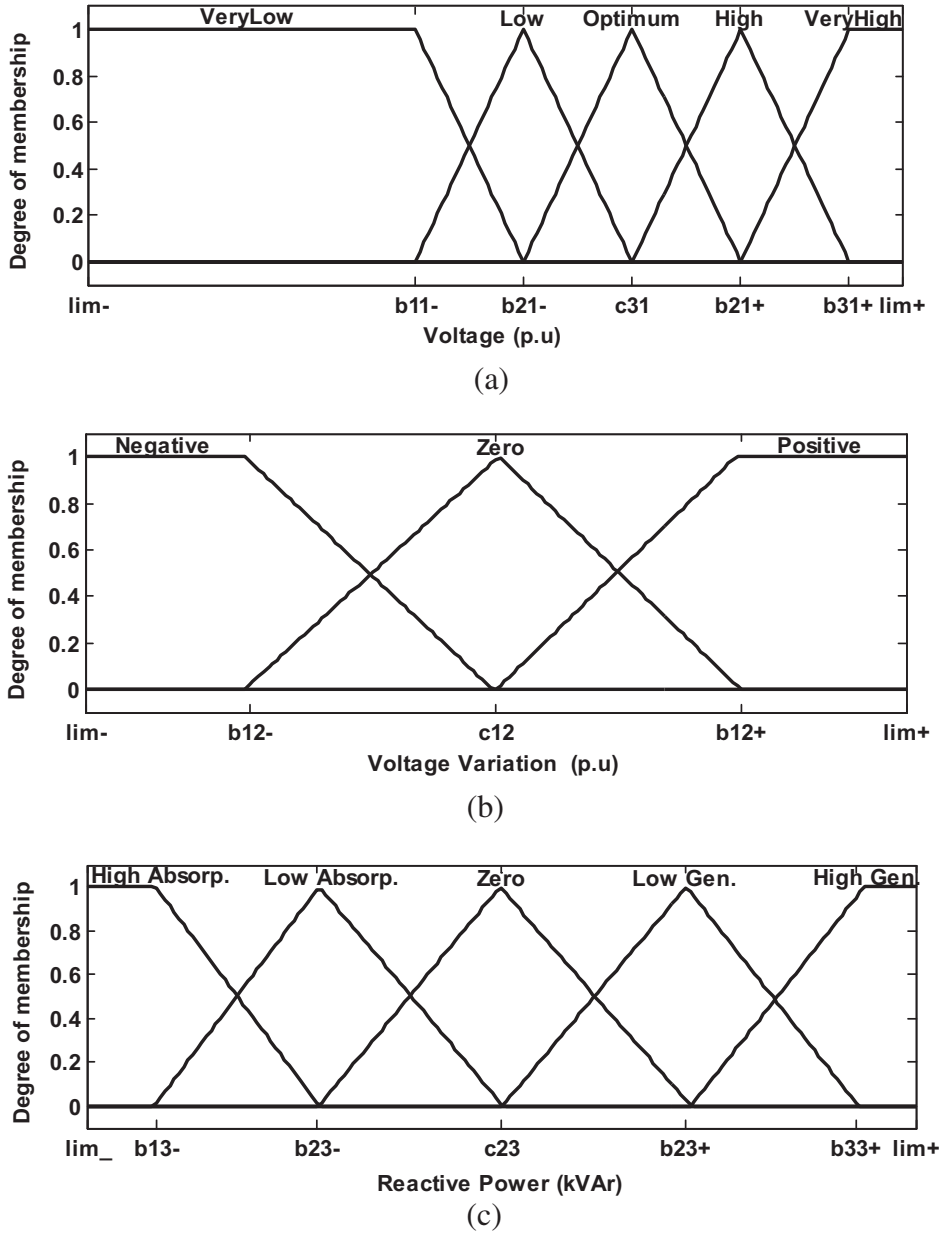

Fig. 4. Fuzzy membership functions: (a) Input 1, (b) Input 2, and (c) Output.

output is different for each DG. The domain of the output membership function is set to cover the reactive power capability of DG. The membership functions are also sum-normal which means that all of the membership functions add up to one in each point of the domain. Sum-normality is desirable for engineers because of easy implementation [25]. The membership functions are then optimized with a mathematical optimization method based on gradient descent algorithm.

To improve the reactive power capability of DFIG wind turbine, in addition to the DFIG stator, the reactive power capability of GSC is also considered and it is added to the reactive power capability of DFIG wind turbine.

Voltage controllers can work independently if they have no mutual interactions on each other, otherwise, they must be coordinated.

3.1.1. Coordination of stator and grid-side converter of DFIG wind turbine in reactive power support

The stator of DFIG can provide larger reactive power capability than GSC. To coordinate DFIG stator and GSC in reactive power support to the grid, the stator is considered as the first and GSC as the second controller [19]. A flowchart of the coordination strategy is shown in Fig. 5. Whenever the stator reaches its reactive power limits, GSC provides the excess reactive power required to regulate the connection bus voltage. The advantage of this coordinated control strategy is that the reactive power capability of GSC can be reserved for fault ride through (FRT) operation. During the fault, the wind turbine crowbar protection is activated and rotor side converter is not able to control reactive power anymore. At these moments, GSC can be controlled to inject reactive power to decrease the voltage dip.

3.1.2. Gradient descent optimization

The gradient descent is an iterative algorithm, which begins from an initial point and moves the point against the slope of an objective function to get to the minimum of that function. This algorithm is used in this paper to adjust the fuzzy membership functions. The object is to improve the voltage profile of the connection bus by controlling the DG reactive power output. The best voltage profile happens when the connection bus voltages during the day have the least possible distances to 1 p.u. Therefore, the objective function is defined as *VR* (voltage regulation) as given in Eq. (20).

$$VR = \frac{1}{N}\sum_{t=1}^{N}|V_{CB}(t) - 1| \tag{20}$$

where N is the number of time steps during 24 h and $V_{CB}(t)$ is the voltage of the connection bus at every time step. Since $V_{CB}(t)$ is related to the output of the fuzzy system, the membership functions have to be optimized to minimize *VR*. The gradient descent algorithm is used to update the membership functions parameters at iteration k as follows:

$$c_{ij}(k+1) = c_{ij}(k) - \eta_{C_{ij}}\frac{\partial VR}{\partial c_{ij}}\bigg|_{C_{ij}(k)} \tag{21}$$

$$b_{ij}^{-}(k+1) = b_{ij}^{-}(k) - \eta_{b_{ij}^{-}}\frac{\partial VR}{\partial b_{ij}^{-}}\bigg|_{b_{ij}^{-}(k)} \tag{22}$$

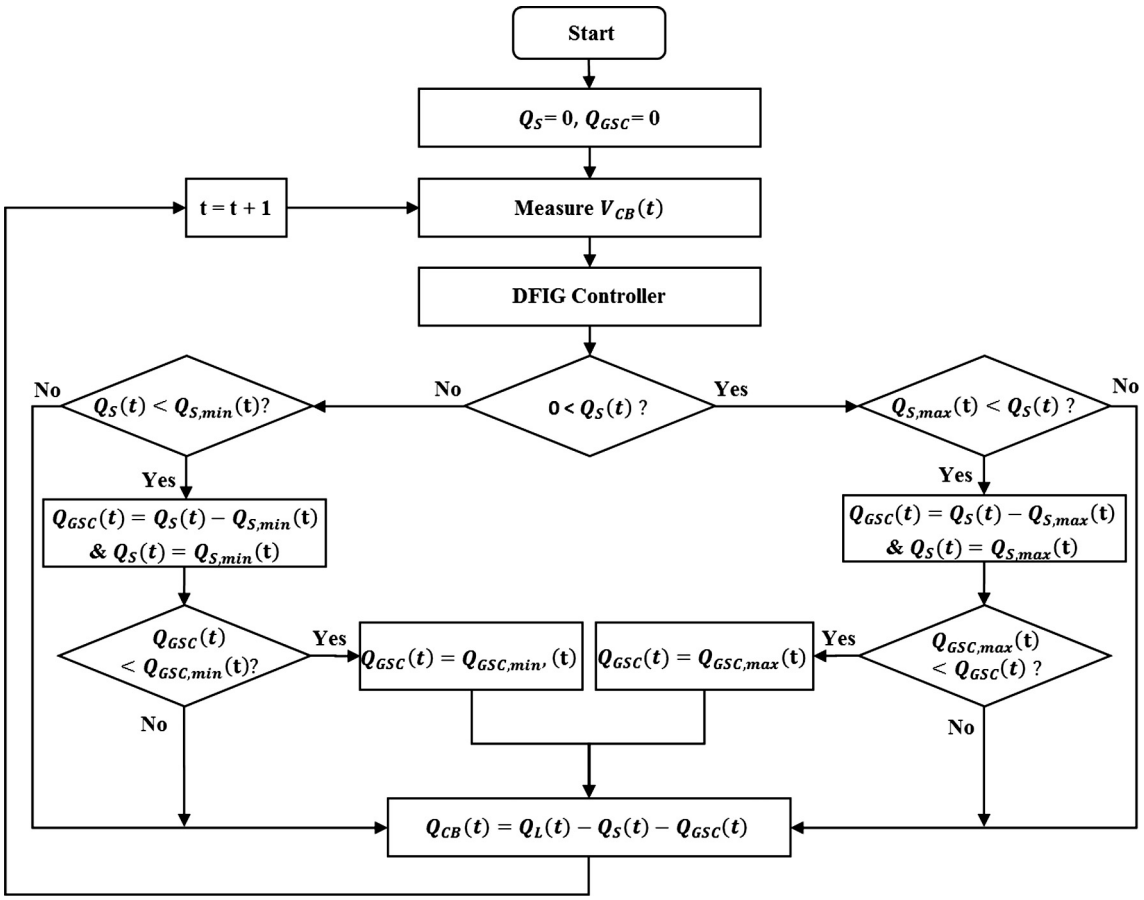

Fig. 5. Flowchart of coordinated reactive power control between DFIG wind turbine and the GSC.

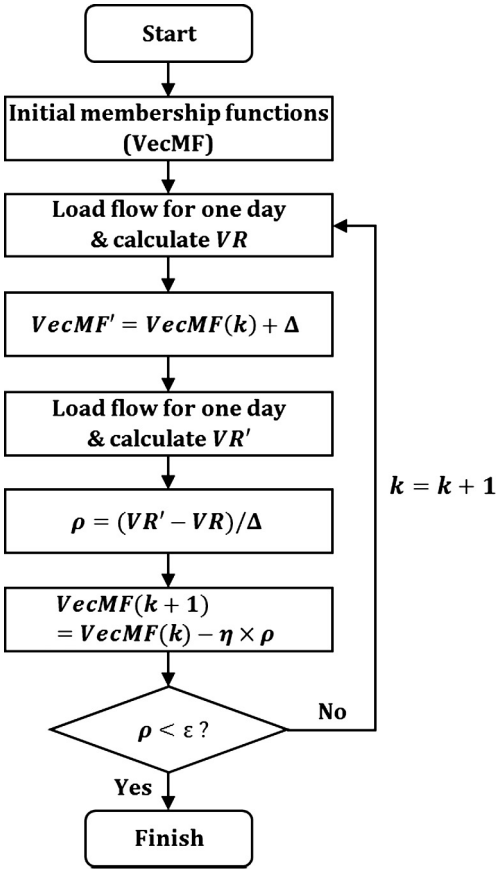

Fig. 6. Flowchart of optimization method.

$$b_{ij}^{+}(k+1) = b_{ij}^{+}(k) - \eta_{b_{ij}^{+}} \left.\frac{\partial VR}{\partial b_{ij}^{+}}\right|_{b_{ij}^{+}(k)} \tag{23}$$

where c_{ij}, b_{ij}^{-} and b_{ij}^{+} are the modal point, lower point and higher point of the ith membership function of jth fuzzy variable, respectively, η is step size of the algorithm for each membership and it can be considered changeable during the iterations but in this paper it is considered a fixed value to avoid the computational complexity of each iteration. Low η values can result in the slow convergence of the algorithm. Therefore, a suitable value of η must be considered for a moderate speed of convergence.

Derivative of VR with respect to c_{ij} ($\rho_{C_{ij}}$), b_{ij}^{-} ($\rho_{b_{ij}^{-}}$), and b_{ij}^{+} ($\rho_{b_{ij}^{+}}$) is estimated by [25]:

$$\rho_{C_{ij}} = \left.\frac{\partial VR}{\partial c_{ij}}\right|_{C_{ij}(k)} \cong \frac{\Delta VR}{\Delta c_{ij}}(k) \tag{24}$$

$$\rho_{b_{ij}^{-}} = \left.\frac{\partial VR}{\partial b_{ij}^{-}}\right|_{b_{ij}^{-}(k)} \cong \frac{\Delta VR}{\Delta b_{ij}^{-}}(k) \tag{25}$$

$$\rho_{b_{ij}^{+}} = \left.\frac{\partial VR}{\partial b_{ij}^{+}}\right|_{b_{ij}^{+}(k)} \cong \frac{\Delta VR}{\Delta b_{ij}^{+}}(k) \tag{26}$$

Therefore, in each iteration ρ is obtained and the membership functions are updated. The gradient descent optimization flowchart is illustrated in Fig. 6. After the membership functions are optimized, the optimized fuzzy systems are used to control the reactive power of the DG units.

3.2. Particle swarm optimization

In this paper, the standard PSO is applied to the distribution system to determine the optimal reactive power of each DG during the day. The PSO is used in different papers to find optimal location, sizing and reactive power of the DGs [3,10,23]. The PSO is a heuristic method based on the movement of swarms. Particles are randomly distributed in the search space and they move to find the global optimum and update their velocities and positions according to Eq. (27) [10].

$$X_i(k) = X_i(k-1) + Vel_i(k) \tag{27}$$

where k is the iteration, and X_i and Vel_i are the position and the velocity of the particle i, respectively, and $Vel_i(k)$ is calculated using the following equation:

$$Vel_i(k) = \omega Vel_i(k) + c_1 r_1 (Pbest_i(k-1) - X_i(k-1)) + c_2 r_2 (Gbest(k-1) - X_i(k-1)) \tag{28}$$

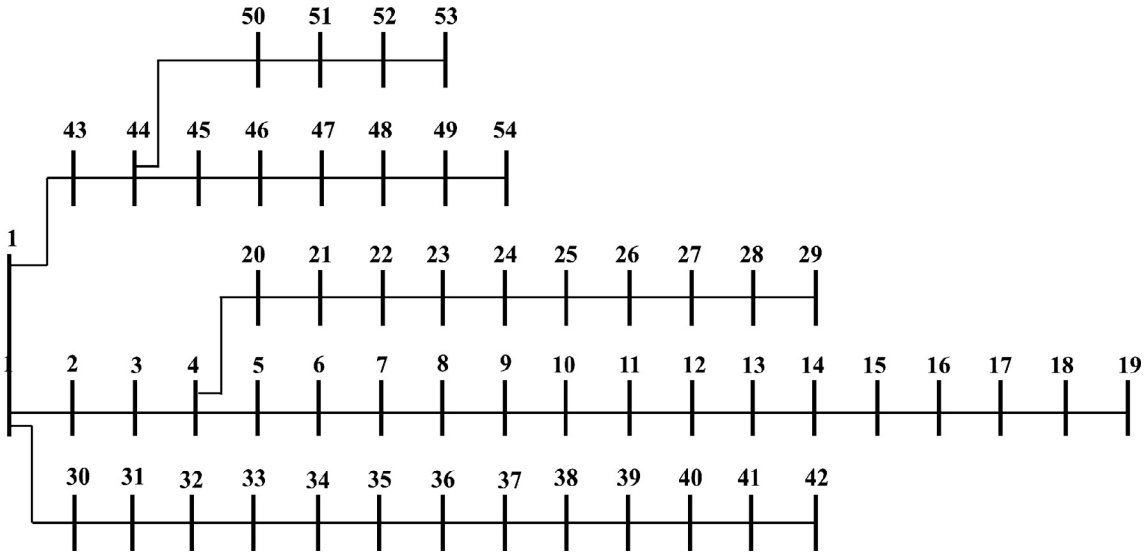

Fig. 7. Single line diagram of 54-bus distribution system.

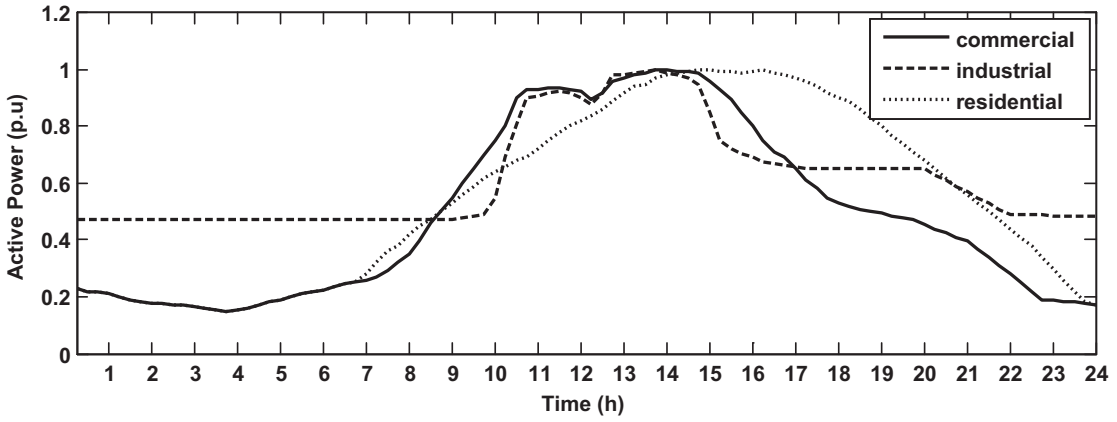

(a)

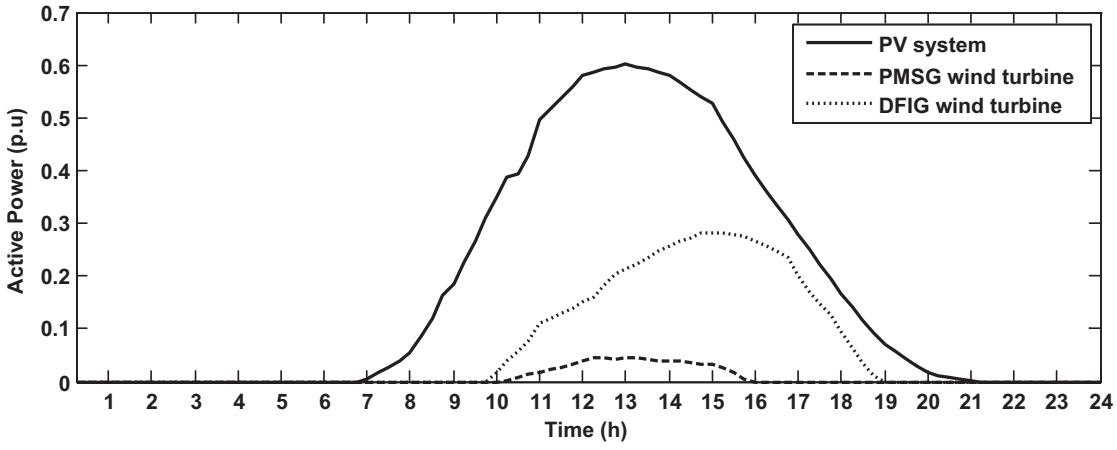

(b)

Fig. 8. Typical active power profiles: (a) load, and (b) DG generation.

Table 3
Comparative study of voltage improvement for different reactive power control methods.

	PV system		PMSG-WT		DFIG-WT	
	Input 1	Output	Input 1	Output	Input 1	Output
VR without voltage control (p.u)	0.242		2.378		1.641	
VR with fuzzy voltage control (p.u)	0.213		1.960		1.272	
VR with optimized fuzzy voltage control (p.u)	0.204	0.196	1.667	1.582	0.989	0.911
VR with centralized voltage control (p.u)	0.070		1.599		0.927	

Table 4
Fuzzy membership functions.

Parameter	Initial values			Optimized values		
	PV system	PMSG WT	DFIG WT	PV system	PMSG WT	DFIG WT
b_{11}^{-}	0.960	0.960	0.960	0.960	0.960	0.962
b_{21}^{-}	0.980	0.980	0.980	0.982	0.992	1.004
c_{31}	1.000	1.000	1.000	0.998	1.003	1.005
b_{21}^{+}	1.020	1.020	1.020	1.012	1.020	1.020
b_{31}^{+}	1.040	1.040	1.040	1.049	1.049	1.049
b_{12}^{-}	−0.030	−0.030	−0.030	−0.030	−0.030	−0.030
c_{12}	0.000	0.000	0.000	0.000	0.000	0.000
b_{12}^{+}	0.030	0.030	0.030	0.030	0.030	0.030
b_{13}^{-}	−1003	−207	−1676	−1107	−198	−1216
b_{23}^{-}	−532	−103	−837	−466	14	571
c_{23}	0	0	0	−33	49	1160
b_{23}^{+}	532	103	837	398	148	1998
b_{33}^{+}	1003	207	1676	1207	259	2095

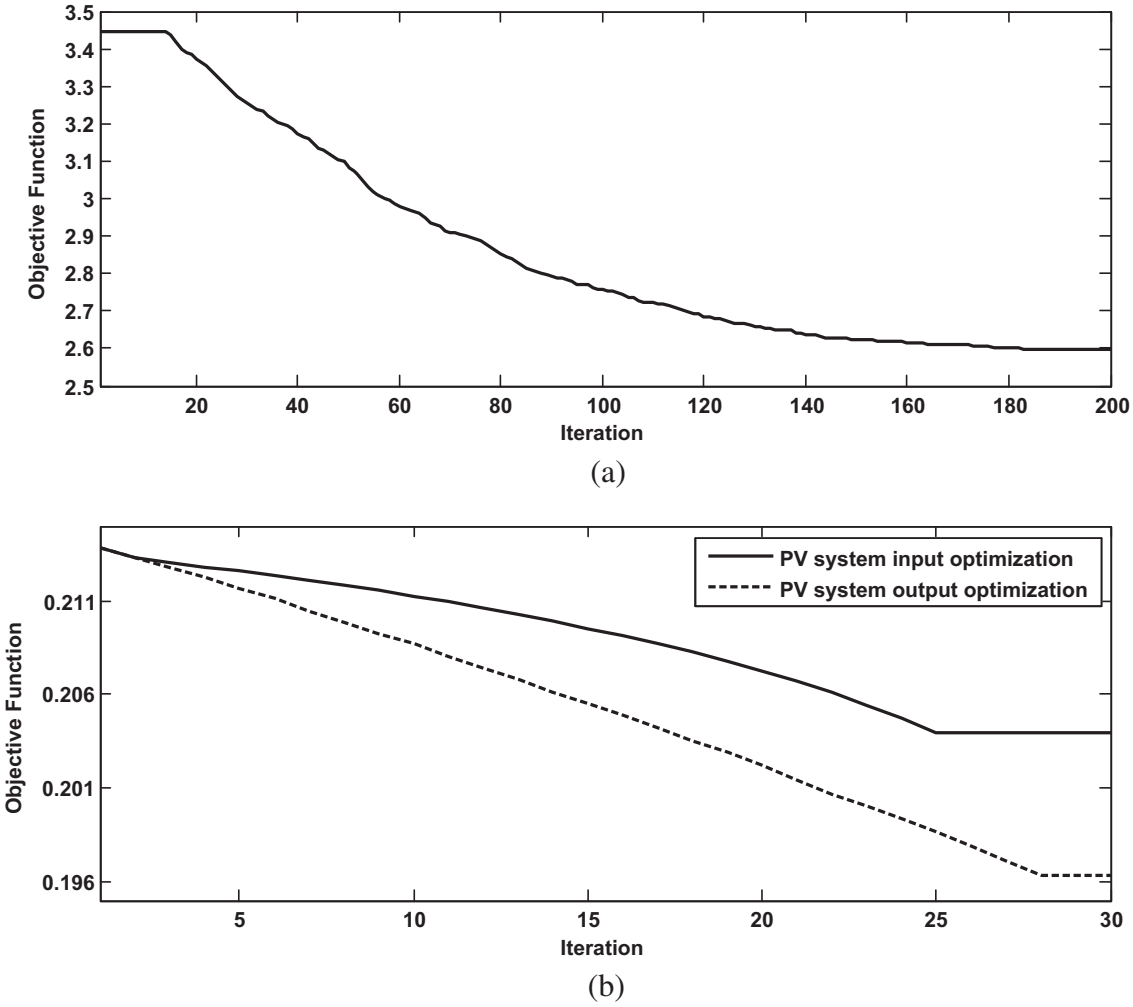

Fig. 9. Convergence curve of the objective function produced by: (a) the PSO, and (b) gradient descent.

Table 5
Comparative study of energy losses during one day for different reactive power control methods.

E_{loss} without voltage control (kWh)	1999
E_{loss} with fuzzy voltage control (kWh)	1773
E_{loss} with optimized fuzzy voltage control (kWh)	1710
E_{loss} with centralized voltage control (kWh)	1763
Q_{loss} without voltage control (kVArh)	2696
Q_{loss} with fuzzy voltage control (kVArh)	2369
Q_{loss} with optimized fuzzy voltage control (kVArh)	2277
Q_{loss} with centralized voltage control (kVArh)	2364

where ω is the inertia weight, c_1 and c_2 are learning factors, r_1 and r_2 are the random numbers between 0 and 1, *Pbest* is personal best position and *Gbest* is the global best position. The objective function (F) is to minimize *VR* at the connection buses of the PV system, PMSG wind turbine, and DFIG wind turbine:

$$\min(F) = \min\left(\sum_{n=1}^{3} VR_n\right) \tag{29}$$

Since there is no interaction between DGs, minimization of F will result in the reduction of *VR* at each DG connection bus.

4. Simulations and results

A real 54-bus distribution system in Sicily of Italy (Fig. 7) with specification given in [4] is used for investigating the performance of the proposed method. Four 20 kV feeders are connected to a transformer with tap position fixed at 1.006 p.u. It is considered that a PV system, a PMSG wind turbine, and a DFIG wind turbine are respectively connected to buses 46, 29 and 3 of the distribution system and the fuzzy system is applied to each DG to regulate its connection bus voltage at 1 p.u. The time steps in all of the simulations are considered 15 min and the simulations are carried out in MATLAB environment on an Intel core i5 CPU 1.7 GHz/4 GB RAM computer system. The 54-bus distribution system has three consumer types including commercial, industrial, and residential (Fig. 8a) [4,15–17]. Consumer type of each bus is given in [4] and load profiles are multiplied by the rated load of the buses to determine the daily load profile of each bus of the distribution grid. Since the load profiles do not influence the validity of the proposed method, the load power factor is assumed to be constant and therefore the reactive power profile is considered similar to the active power daily load curve [4,15–17]. In Fig. 8b, daily DG generations are depicted, where the per-unit base is the nominal active power of each DG. PV system generation is the hourly average power obtained from a real system in Catania in Sicily [26] and wind turbines generation profiles are calculated based on hourly average wind speeds of Catania and Messina both in Sicily [27]. The generation profile calculations are presented in Appendix A. Also, calculation of slip of the DFIG wind turbine is given in Appendix B.

The proposed optimization method is performed in the distribution system to obtain the optimal membership functions. Each

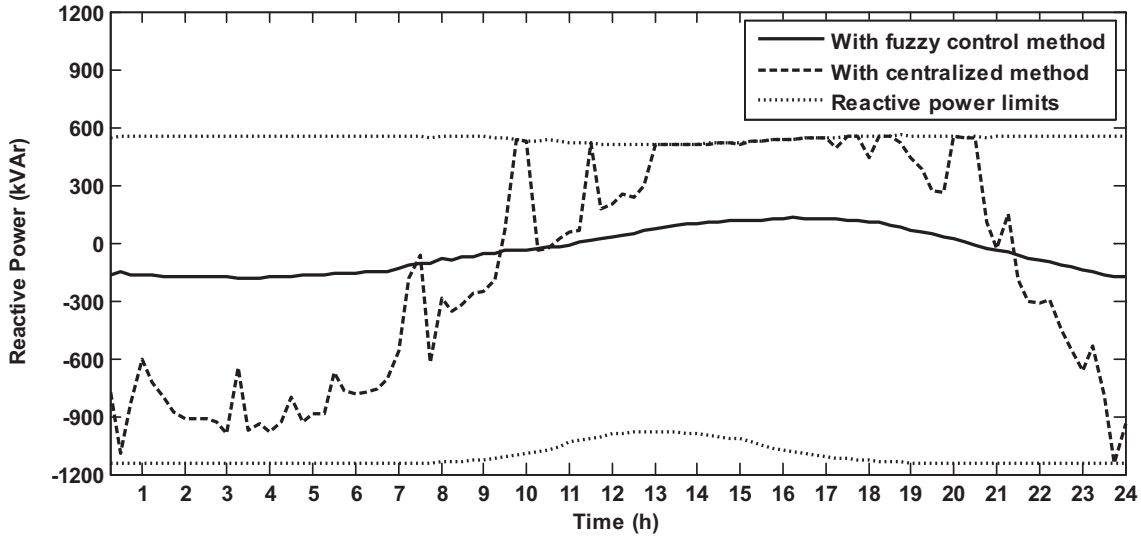

(a)

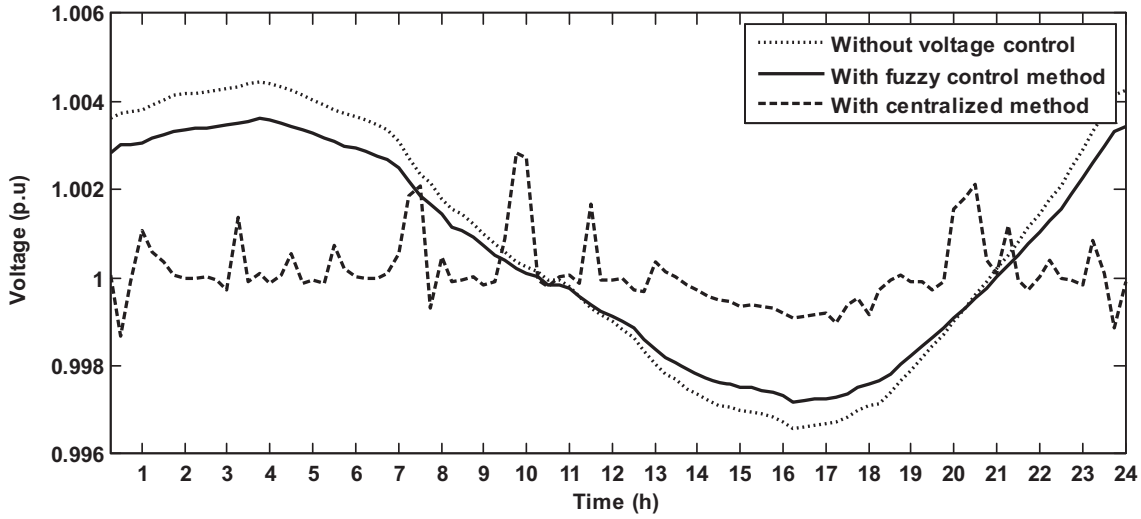

(b)

Fig. 10. Performance of PV system: (a) reactive power output, and (b) bus voltage.

fuzzy system is optimized independently of other systems and also input 1 and output membership functions are optimized separately. For input optimization, a value of 0.0003 and for output optimization values between 30,000 and 500,000 are suitable for η. Δ is considered 0.001 and 5 for input and output optimization, respectively. The initial membership functions are considered in such a way that the area under the membership functions is almost equal. In this way, probable oscillations in the output of the fuzzy system are avoided. The initial values are then adjusted by the gradient descent algorithm. Before DGs participate in the voltage control, *VR* is 0.242 p.u, 2.378 p.u, and 1.641 p.u for PV system, the PMSG wind turbine, and DFIG wind turbine respectively. After the reactive power control of DGs, voltage profiles of DG buses are improved thus *VR* is reduced to 0.213 p.u, 1.960 p.u, and 1.272 p.u, respectively as shown in Table 3. The optimization of fuzzy system has resulted in a decrease in *VR*. It can be seen that fuzzy output optimization is more effective than fuzzy input optimization and *VR* is decreased to 0.196 p.u, 1.582 p.u, and 0.911 p.u, respectively. From now on DG fuzzy systems with the optimized outputs are considered in all of the simulations. The membership functions parameters with and without optimization are given in Table 4. To verify the performance of the proposed method in the voltage control, the PSO is also adopted. The quantity of variables is considered 288 in the PSO. Population size is chosen 20. ω is considered 0.2 and $c_1 = c_2 = 2$. The PSO and the GDA converged to the optimal solution within 200 iterations and 23–38 iterations, respectively. In Fig. 9, convergence curve of the objective function produced by the PSO algorithm and the gradient descent algorithm for PV fuzzy system optimization is illustrated. *VR* obtained by the centralized method is 0.070 p.u, 1.599 p.u, and 0.927 p.u for PV system, the PMSG wind turbine, and DFIG wind turbine, respectively, As shown in Table 3, the resulting *VR* is near to the *VR* obtained by the proposed method, which proves that the fuzzy logic-based method has controlled the voltage very well and the GDA has been successful in the adjustment of the fuzzy membership functions. In addition to voltage improvement, both of the centralized and decentralized methods also reduce active and reactive energy consumed by the lines (E_{loss}, and Q_{loss}), as shown in

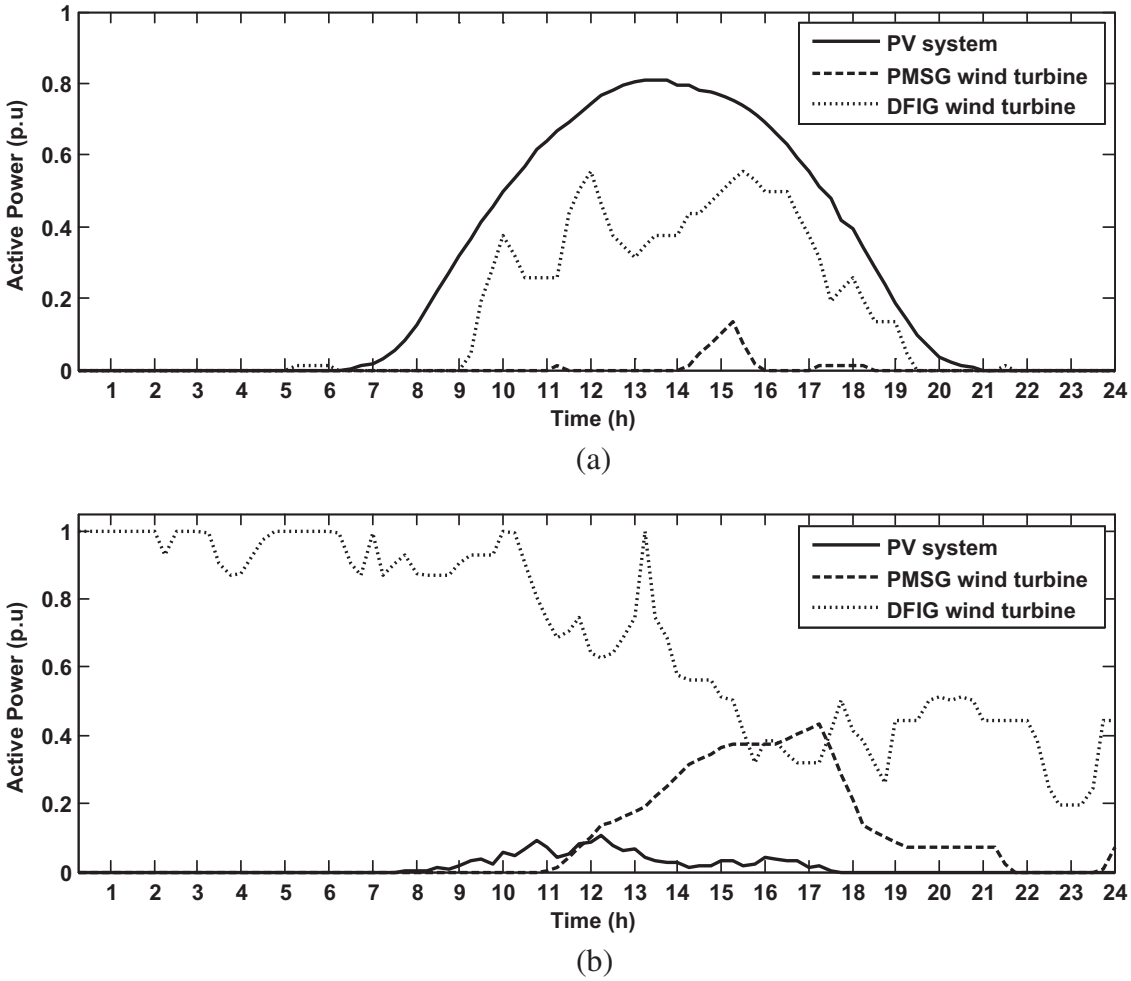

Fig. 11. DG generation in different seasons: (a) in a summer day, (b) in a winter day.

Table 5. The proposed decentralized method is more successful in the reduction of E_{loss} and Q_{loss} than the centralized method and decreases E_{loss} and Q_{loss} to 1710 kWh and 2277 kVArh, respectively.

Reactive power and bus voltage of PV system is depicted in Fig. 10. Fuzzy system controls the reactive power output of the PV system according to voltage variation of the DG connection bus. Before 11:00 AM and after 9:00 PM, the voltage is over 1 p.u, therefore PV system absorbs reactive power to decrease voltage. At other times, PV system produces reactive power to increase voltage. Fig. 10 shows that fuzzy system is tracking the centralized method very well and reactive power output of the fuzzy system is gradually changing according to the voltage variations. As seen in Fig. 10a, the reactive power consumed by PV system in the proposed method is less than the reactive power consumption in the centralized method. At peak load hours, 1:00–5:00 PM, PV system's reactive power output reaches its upper limit in the centralized method and the DG can't produce more reactive power than its capability.

To verify that the resulting optimized fuzzy system is capable of voltage control with different load and generation profiles, a sunny day in the summer and a cloudy day in the winter of Catania and Messina are considered. The generation profiles are obtained from real data in [26,28] (Fig. 11). The load profiles are considered as given in [15] (Fig. 12). The simulation results in Table 6 indicate that the fuzzy system is able to operate in different weather conditions and also in different load profiles. *VR* without reactive power control of the PMSG wind turbine is 1.744 p.u and 1.771 p.u in the summer and the winter day, respectively. With reactive power control, *VR* is reduced to 1.178 p.u in the summer day and 1.405 p.u in the winter day. The PMSG wind turbine bus voltage is depicted in Fig. 13, which shows the voltage profile improvement and the good performance of the PMSG wind turbine fuzzy system in providing reactive power. At peak hours, when the voltage is below 0.98 p.u, the wind turbine produces its maximum reactive power to increase the bus voltage.

PV systems and wind turbines provide fast control actions, therefore, when they contribute to reactive power control, they can simultaneously respond to voltage variations and there is a possibility that their control actions lead to operational conflicts. To elucidate the problem, it is considered that DFIG wind turbine and PV system are connected to bus 26 and 27 and each DG is regulating its bus voltage at 1 p.u. At 1:00 AM, the voltage of bus 26 and 27 are 0.988 p.u, therefore, both wind turbine and PV system simultaneously react to voltage dip and they inject 1176 kVAr and 351 kVAr reactive power, respectively to increase the voltage. The voltage is then increased to 1.003 p.u. The resulting voltage is above 1 p.u, so DGs have to absorb reactive power to regulate the voltage. This conflict can repeat again and cause additional DG reactive power production. In this case, it is required to coordinate DGs. If a time delay is applied to the DG farther from the substation, the conflict can be mitigated. As given in Table 7, at first DFIG wind turbine reacts to voltage variation and produces 1176 kVAr reactive power. Consequently, the bus voltage of both DGs increases to 0.999 p.u. Since the voltage is regulated, the delayed

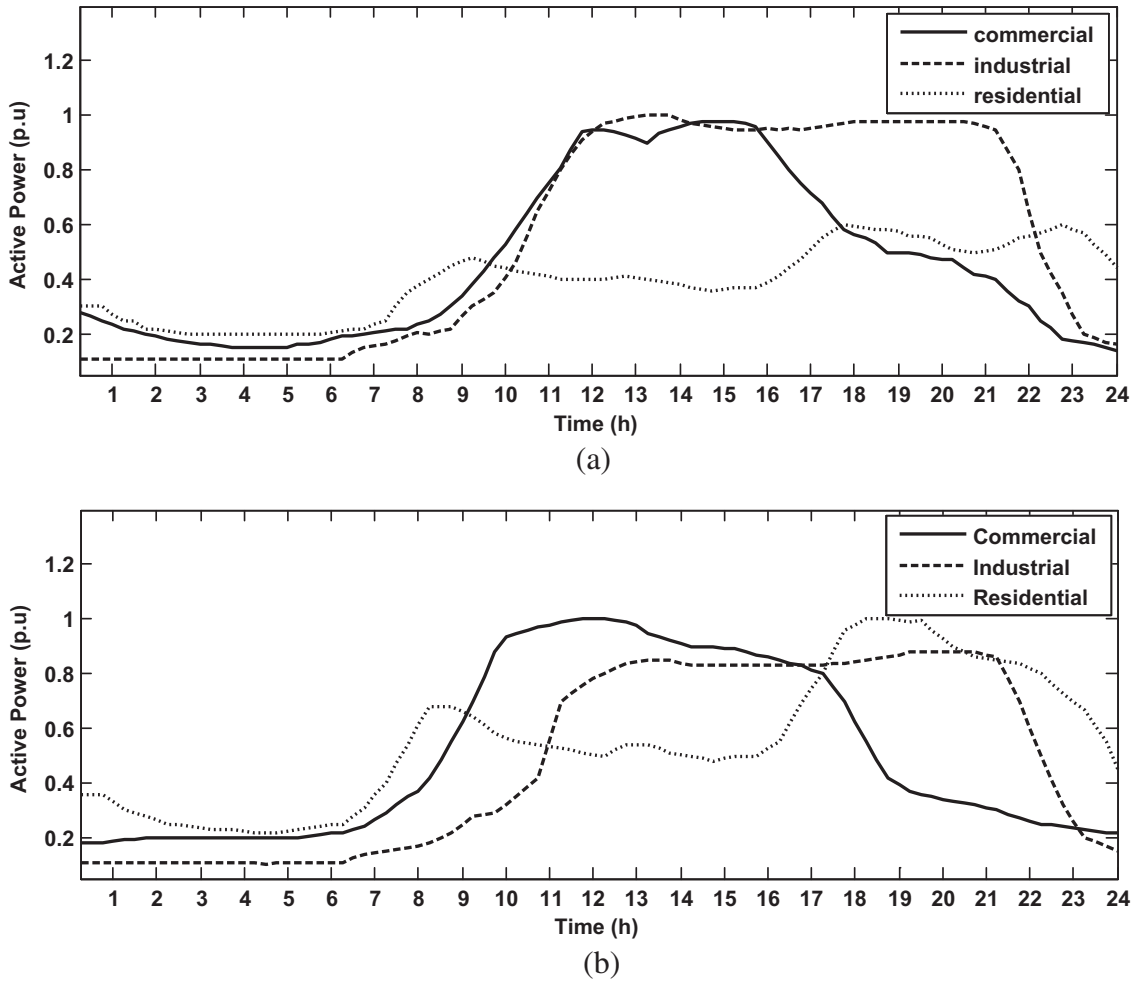

Fig. 12. Load demand profiles in different seasons: (a) in a summer day, and (b) in a winter day.

Table 6
Simulation results in the summer day and the winter day.

	PV system	PMSG WT	DFIG WT
VR without voltage control in the summer day (p.u)	0.254	1.744	1.205
VR with voltage control in the summer day (p.u)	0.201	1.178	0.857
VR without voltage control in the winter day (p.u)	0.199	1.771	1.250
VR with voltage control in the winter day (p.u)	0.159	1.405	0.972

PV control system doesn't participate in reactive power control. The total amount of reactive power produced by two DGs in this strategy is 351 kVAr less than in the first scenario with simultaneous operation of DGs. When a new DG is utilized to participate in voltage control, it must be coordinated with other regulating devices if they have operational conflicts. In [29], it is explained that mutual interactions between DGs can result in overvoltage. According to this problem, sometimes it might be necessary to change the reference setting of the fuzzy system.

To test the function of the optimized fuzzy control system in another power grid, it is considered that a PV system, a PMSG wind turbine, and a DFIG wind turbine are installed at bus 19, 6 and 3 of the IEEE 33 bus radial distribution test system (Fig. 14). The DG generations in the winter day and the industrial load profile depicted in Fig. 12b are applied to the system and the fuzzy-based method is implemented in the distribution system. The results are given in Table 8, which shows that *VR* at each DG bus is reduced after the voltage control and the fuzzy system worked good in a different distribution system. However, it is recommended to tune the fuzzy system if the DG is connected to the buses with high sensitivity of voltage to reactive power, because it might result in output oscillation of the fuzzy system.

Fig. 15a, illustrates the voltage dip of 0.982 p.u at bus 3. After applying fuzzy based voltage control method, DFIG wind turbine participates in reactive power control and improves the voltage dip to 0.986 p.u. Except for hours between 10:30 PM and 12:00 PM, DFIG wind turbine is always at its upper reactive power limit (Fig. 15b). From Figs. 11b and 15b it can be seen that the upper reactive power limit of DFIG wind turbine is changing rapidly with DG active power variation. To increase the reactive power capability of DFIG wind turbine, it is considered that the GSC is also participating in voltage control. Whenever the DFIG wind turbine reaches its reactive power limits, the GSC contributes in providing the required reactive power (Fig. 16). At peak hours, the GSC produces its maximum reactive power. With GSC support voltage profiles are improved as seen in Fig. 15a and Table 8. The GSC support of reactive power, also resulted in voltage improvement of the bus 6, where the PMSG wind turbine is installed (Fig. 17a). Before reactive power control of DGs, the voltage at bus 6 is below 0.95 p.u at several hours. Therefore, the PMSG wind turbine injects reactive power to its full capacity to mitigate the voltage dip. After the voltage control, there are still hours with

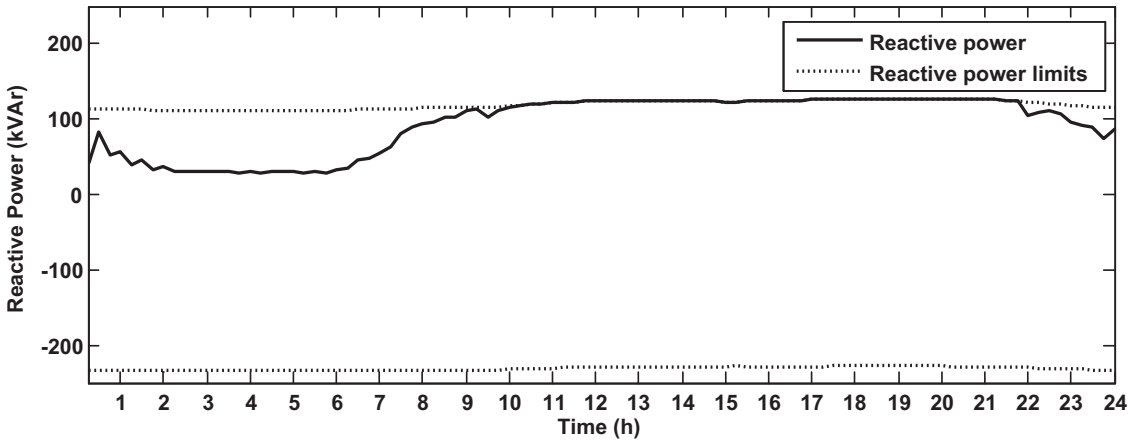

(a)

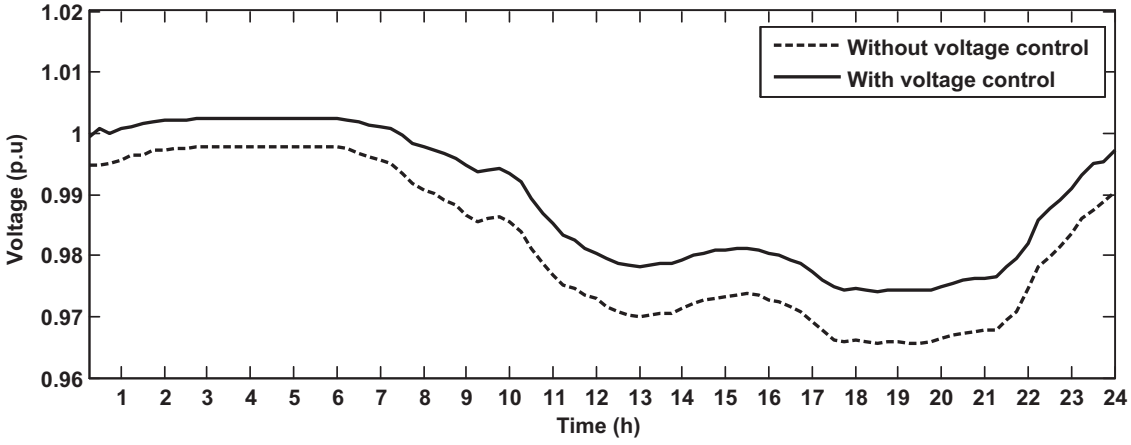

(b)

Fig. 13. Performance of the PMSG wind turbine in a summer day: (a) reactive power output, and (b) bus voltage.

Table 7
Performance of DGs with and without coordination.

	PV system	DFIG WT
Bus voltage without voltage control (p.u)	0.988	0.988
Reactive power without coordinated voltage control (kVAr)	351	1176
Bus voltage without coordinated voltage control (p.u)	1.003	1.003
Reactive power with coordinated voltage control (kVAr)	0	1176
Bus voltage with coordinated voltage control (p.u)	0.999	0.999

Table 8
Simulations results in the IEEE 33-bus distribution system.

	PV system	PMSG WT	DFIG WT
VR without voltage control (p.u)	0.168	2.537	0.841
VR with voltage control (p.u)	0.140	2.310	0.757
VR with GSC support (p.u)	0.136	2.268	0.732

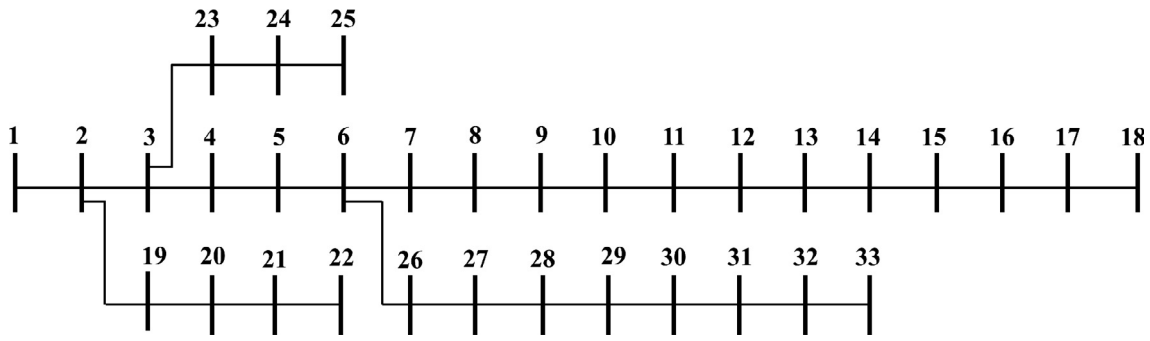

Fig. 14. Single line diagram of the IEEE 33-bus distribution system.

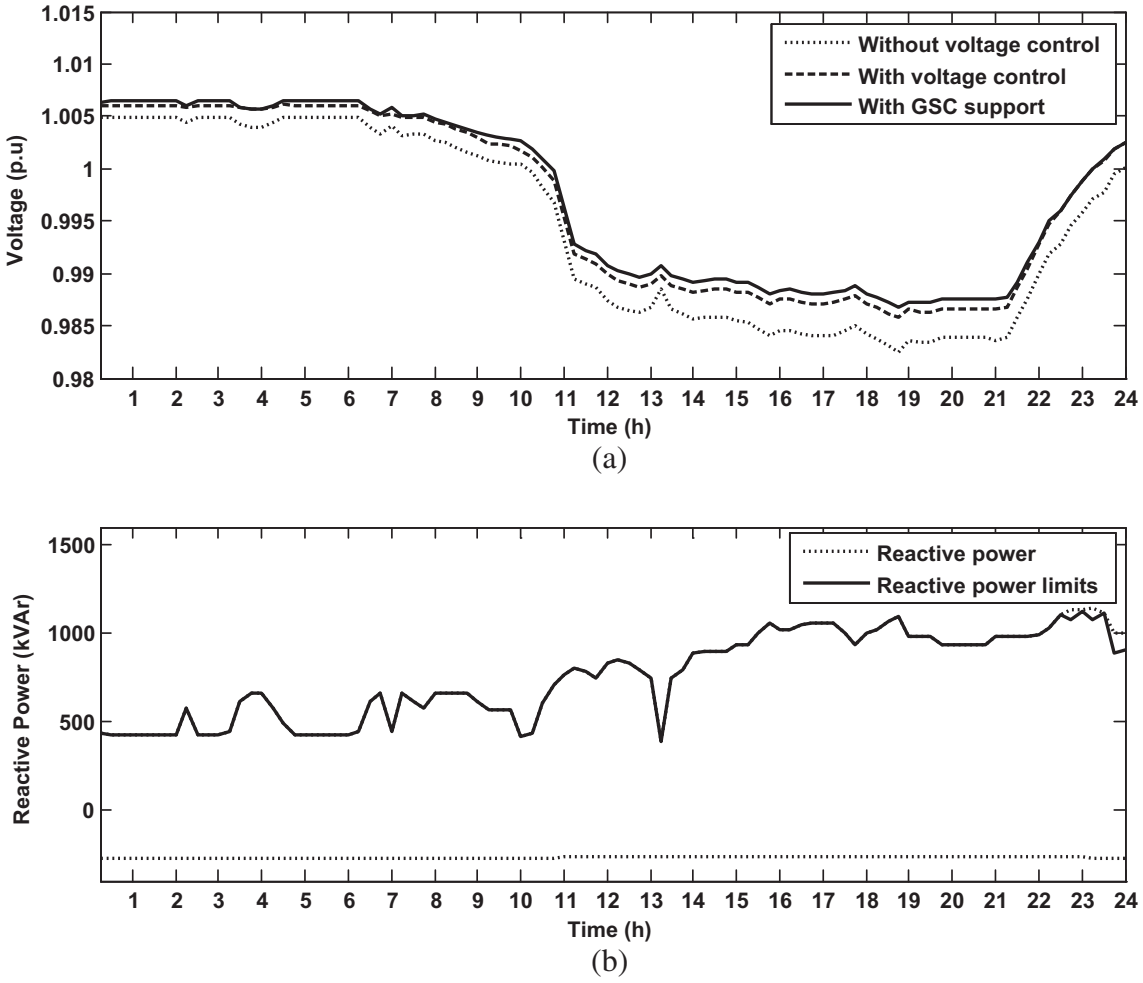

Fig. 15. Performance of DFIG wind turbine: (a) bus voltage, and (b) reactive power output.

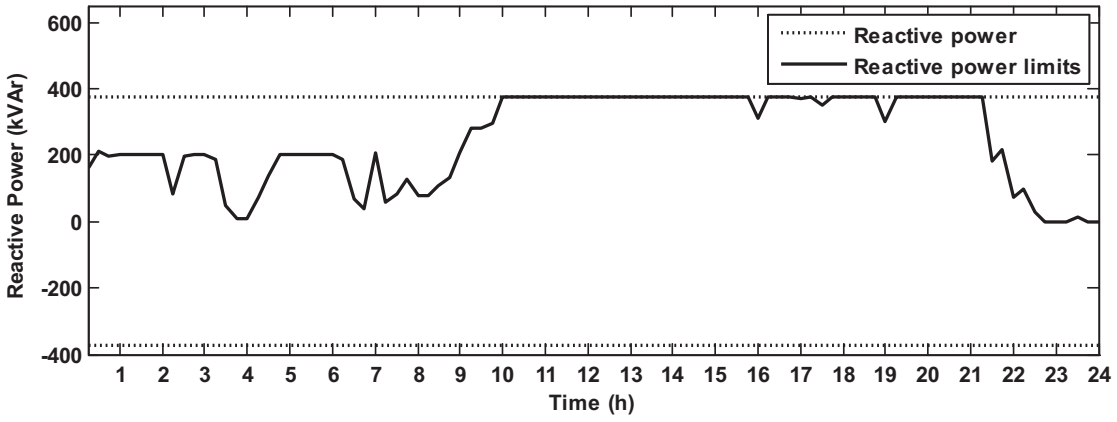

Fig. 16. Reactive power output of the GSC.

voltages lower than 0.95 p.u, but after the GSC support, bus voltage at all hours increases to more than 0.95 p.u.

5. Conclusions

In this paper, a decentralized method is used for reactive power control of PV systems and wind turbines with the aim to regulate DG bus voltage. The proposed method is based on a fuzzy system that its membership functions are optimized by the gradient descent algorithm. The reactive power capability of PV systems, PMSG wind turbines, and DFIG wind turbines are considered in the voltage control. The simulations are conducted in a real 54 bus distribution system during a typical day, a summer day and a winter day. To evaluate the performance of the fuzzy control system, a centralized method based on the PSO is also performed to obtain the optimal reactive power output of the DGs. The fuzzy control

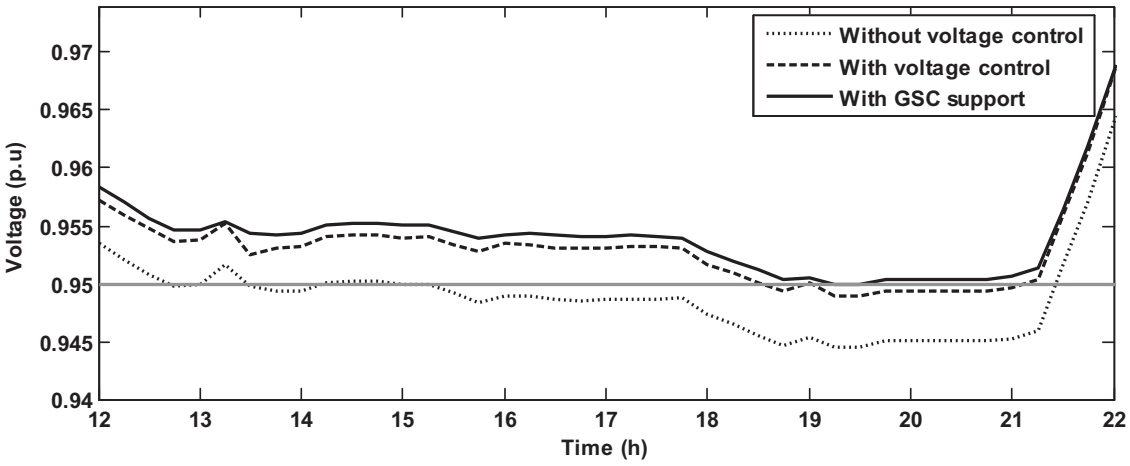

(a)

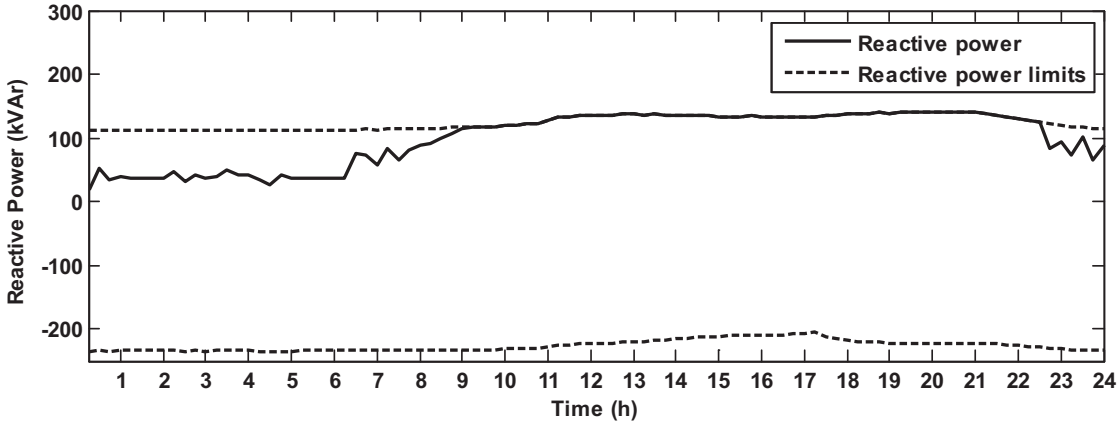

(b)

Fig. 17. Performance of the PMSG wind turbine: (a) bus voltage, and (b) reactive power output.

system is also applied to the IEEE 33 bus distribution network to show the robustness of the proposed method. A scenario in which an unwanted conflict appears in the DGs' function is defined in detail and then a strategy is presented to resolve the situation. To increase the reactive power support of DFIG wind turbine, a strategy for coordination of the DFIG stator and the GSC is also proposed. The simulations show the following results:

- The proposed method based on the fuzzy logic successfully improves the voltage profile through using DGs reactive power capability. The comparison of the results obtained by the fuzzy control system with the centralized method, shows that the reactive power output obtained by the proposed method is close to the optimum solution determined by the centralized method. The centralized method is able to find optimal reactive power more precisely in some cases whereas, the proposed fuzzy system provides a gentler action control.
- The centralized method requires data of all DGs in the distribution system, while the proposed method is implemented on each DG separately and requires voltage variation of the bus at which the DG is connected. Also, the gradient descent optimization used in the proposed method converges in fewer iterations than the PSO algorithm used in the centralized method. Therefore, the proposed method is fast and can be easily implemented.
- When the fuzzy parameters are adjusted by the optimization algorithm, the proposed method is able to control the voltage online. The fuzzy control systems is very robust and it has high tolerances for changes in the inputs. Therefore, the proposed method has a good performance when the load profile or DG generations are changed, whereas the PSO algorithm of the centralized method must be run again to determine the reactive power output of DGs.
- Since the fuzzy method is implemented and optimized for each DG separately and without considering other DGs operation, mutual interactions between DGs are possible in the distribution systems. Simultaneous responses of DGs can be mitigated by considering time delays for each DG's control system. However, some operational conflicts cannot be avoided by this strategy and the DG's target voltage has to be modified.

Appendix A

As given in [9], wind turbine generation can be calculated from wind speed (V) by the piecewise linear function as given below:

$$P_{DG} = \begin{cases} 0, & \forall V \leqslant V_I \\ \left(\frac{V-V_I}{V_R-V_I}\right)P_R, & \forall V_I < V < V_R \\ P_R, & \forall V \geqslant V_R \end{cases} \quad (30)$$

where V_I and V_R are cut-in and rated wind speed of wind turbine, respectively and P_r is the rated active power of wind turbine.

Appendix B

Slip of the DFIG wind turbine is obtained similarly to the diagrams given in [27]:

$$S = \begin{cases} 1, & \forall P_{DG} = 0 \\ S_{max}, & \forall 0 < P_{DG} \leqslant P_1 \\ \frac{(S_{max} - S_{min}) \times (P_{DG} - P_2)}{(P_1 - P_2)} + S_{min}, & \forall P_1 < P_{DG} \leqslant P_2 \\ S_{min}, & \forall P_{DG} > P_2 \end{cases} \quad (31)$$

where P_1 and P_2 are given as follows:

$$P_1 = \frac{(5.5 - V_I)}{(V_R - V_I)} \quad (32)$$

$$P_2 = \frac{(11 - V_I)}{(V_R - V_I)} \quad (33)$$

References

[1] Sawin JL, Sverrisson F, Chawla K, Lins C, McCrone A, et al. Renewables 2014 global status report. Renewable energy policy network for the 21st century (REN21); 2014.

[2] Davda AT, Azzopardi B, Parekh BR, Desai MD. Dispersed generation enable loss reduction and voltage profile improvement in distribution network; case study, Gujarat, India. IEEE Trans Power Syst 2014;29:1242–9.

[3] Kayal P, Chanda CK. Optimal mix of solar and wind distributed generations considering performance improvement of electrical distribution network. Renew Energy 2015;75:173–86.

[4] Calderaro V, Galdi V, Lamberti F, Piccolo A. A smart strategy for voltage control ancillary service in distribution networks. IEEE Trans Power Syst 2015;30:494–502.

[5] SMA Solar Technology AG. Description of the operating parameters: SUNNY TRIPOWER 60. STP60-10-Parameter-TI-en-10, Version 1.0.

[6] Varma RK, Khadkikar V, Seethapathy R. Nighttime application of PV solar farm as STATCOM to regulate grid voltage. IEEE Trans Energy Convers 2009;24:983–5.

[7] General Electric Company. Wind power plant performance. GEA-14595 (05/06). Available: <www.ge-energy.com/wind>.

[8] Siemens Wind Power. Siemens reactive power at no wind: support the grid even when the wind is not blowing. E50001-D530-A123-X-4A00, Denmark; 2012. Available: <www.siemens.com/wind>.

[9] Ullah NR, Bhattacharya K, Thiringer T. Wind farms as reactive power ancillary service providers; technical and economic issues. IEEE Trans Energy Convers 2009;24:661–72.

[10] Zhao J, Li X, Hao J, Lu J. Reactive power control of wind farm made up with doubly fed induction generators in distribution system. Electr Power Syst Res 2010;80:698–706.

[11] Tonkoski R, Lopes LAC. Impact of active power curtailment on overvoltage prevention and energy production of PV inverters connected to low voltage residential feeders. Renew Energy 2011;36:3566–74.

[12] Jahangiri P, Aliprantis DC. Distributed Volt/VAr control by PV inverters. IEEE Trans Power Syst 2013;28:3429–39.

[13] Oshiro M, Tanaka K, Senjyu T, Toma S, Yona A, Saber AY, et al. Optimal voltage control in distribution systems using PV generators. Int J Electr Power Energy Syst 2011;33:485–92.

[14] Jashfar S, Esmaeili S. Volt/var/THD control in distribution networks considering reactive power capability of solar energy conversion. Int J Electr Power Energy Syst 2014;60:221–33.

[15] Calderaro V, Conio G, Galdi V, Massa G, Piccolo A. Optimal decentralized voltage control for distribution systems with inverter-based distributed generators. IEEE Trans Power Syst 2014;29:230–41.

[16] Calderaro V, Galdi V, Lamberti F, Piccolo A. Coordinated local reactive power control in smart distribution grids for voltage regulation using sensitivity method to maximize active power. J Electr Syst 2013;9–4:481–93.

[17] Calderaro V, Conio G, Galdi V, Piccolo A. Reactive power control for improving voltage profiles: a comparison between two decentralized approaches. Electr Power Syst Res 2012;83:247–54.

[18] Amaris H, Alonso M. Coordinated reactive power management in power networks with wind turbines and FACTS devices. Energy Convers Manage 2011;52:2575–86.

[19] Meegahapola L, Littler T, Perera S. Capability curve based enhanced reactive power control strategy for stability enhancement and network voltage management. Int J Electr Power Energy Syst 2013;52:96–106.

[20] Ranamuka D, Agalgaonkar AP, Muttaqi KM. Online voltage control in distribution systems with multiple voltage regulating devices. IEEE Trans Sustain Energy 2014;5:617–28.

[21] Di Fazio Anna R, Fusco Giuseppe, Russo Mario. Decentralized control of distributed generation for voltage profile optimization in smart feeders. IEEE Trans Smart Grid 2013;4:1586–96.

[22] Tian J, Su C, Chen Z. Reactive power capability of the wind turbine with Doubly Fed Induction Generator. In: IECON 2013-39th annual conference of the IEEE on Industrial Electronics Society; 2013. p. 5312–7.

[23] Karimyan P, Gharehpetian GB, Abedi M, Gavili A. Long term scheduling for optimal allocation and sizing of DG unit considering load variations and DG type. Int J Electr Power Energy Syst 2014;54:277–87.

[24] Duong Q, Hung Q, Mithulananthan N, Lee Kwang Y. Optimal placement of dispatchable and nondispatchable renewable DG units in distribution networks for minimizing energy loss. Electr Power Energy Syst 2014;55:179–86.

[25] Simon D. Sum normal optimization of fuzzy membership functions. Int J Uncertain, Fuzz Knowl-Based Syst 2002;10:363–84.

[26] SMA sunny portal [Online]. Publicly available PV systems. GolGP SolarHelios PV system. Available: <www.sunnyportal.com>.

[27] Bivona S, Burlon R, Leone C. Hourly wind speed analysis in Sicily. Renew Energy 2003;28:1371–85.

[28] Wunderground historical weather [Online]. Available: <www.wunderground.com/history>.

[29] Li Huijuan, xing Fang, Xu Yan, Tom Rizy D, Adhikari Sarina. Autonomous and adaptive voltage control using multiple distributed energy resources. IEEE Trans Power Syst 2013;28:718–30.